Performance of Phase Retrieval via Phaselift and Quadratic Inversion in Circular Scanning Case

Raffaele Moretta and Rocco Pierri

***Abstract*— The reconstruction of the field radiated by a source from square amplitude-only data falls into the realm of *phase retrieval*. In this paper, we tackle the phase retrieval with two different approaches. The first one is based on a convex optimization problem called *PhaseLift*. The latter exploits the *lifting technique* to recast phase retrieval as a linear problem with an increased number of unknowns and then, because the linear problem is highly undetermined, it adds further constraints (based on the mathematical properties of the solution) to estimate it. The second approach formulates phase retrieval as a least squares problem and, therefore, it requires to tackle the minimization of a quartic functional which will be carried out by applying a gradient descent method. In the second part of this paper, in order to corroborate the effectiveness of both approaches, we present the numerical results. Afterward, we provide a comparison between the two methods and finally, we emphasize how the ratio between the number of independent data and the number of unknowns impacts on the performance in both approaches.**

***Index Terms*— Independent data, phaselift, phase retrieval, quartic functional.**

I. Introduction

THE problem of recovering a signal from phaseless measurements of its linear transformation is called *phase retrieval* [1]. This problem belongs to the class of nonlinear ill-posed problems and (in its quadratic formulation) it consists of finding the unknown vector $\underline{x}$ from the set of quadratic equations

$$\left|\underline{a}_m^H \underline{x}\right|^2 = b_m \quad \forall m \in \{1, \ldots, M\} \tag{1}$$

where $\underline{a}_m^H$ indicates the conjugate transpose of the vector $\underline{a}_m$.

Phase retrieval arises not only in inverse electromagnetic problems [4]–[13] but also in optics [14], [15], in electron microscopy [16], in X-ray crystallography [17], [18], in quantum mechanics, in astronomy [19], and in many other fields of sciences and engineering [20], [21]. In general, this matter is tackled when phase measurements cannot be performed as happens at high frequencies. Furthermore, even when they are feasible, it is worth bearing in mind that the instrumentation which measures signal amplitude only is less expensive.

Manuscript received January 29, 2019; revised May 31, 2019; accepted July 7, 2019. Date of publication July 26, 2019; date of current version November 27, 2019. This work was supported by the European Union and the Italian Ministry of University and Research funding through "Programma Operativo Nazionale Ricerca e Innovazione 2014–2020." *(Corresponding author: Raffaele Moretta.)*

The authors are with the Department of Engineering, University of Campania Luigi Vanvitelli, 81031 Aversa, Italy (e-mail: raffaele.moretta@unicampania.it).

Color versions of one or more of the figures in this article are available online at http://ieeexplore.ieee.org.

Digital Object Identifier 10.1109/TAP.2019.2930127

Given the relevance of the matter and the numerous applications in which phase retrieval is involved, it is useful to study the existence of a solution, the uniqueness of the solution, and the choice of an efficient procedure to estimate it.

The existence of a solution is related to the presence of noise in data. In the presence of corrupted data, the solution may not exist but it is always possible to define a generalized solution in the Tikhonov sense such as the global minimum of the functional which evaluates the distance between data provided by the model and observed data [22].

With regard to the uniqueness of the solution, obviously, the set of equations expressed by (1) does not have a unique solution due to the presence of some trivial ambiguities. The latter is caused by a multiplication with a global phase ($e^{j\alpha}$ with $\alpha \in [-\pi, \pi]$), by the conjugation ($\underline{x}^*$), and, in the case of intensity measurements of Fourier, by a shift of the unknown signal on its support. For these reasons, in the absence of further *a priori* information, the solution of the phase retrieval problem generally is not unique but it can be unique up to the above-mentioned ambiguities. Obviously, if the number of independent data is not high enough, the solution is not unique even neglecting such trivial ambiguities (see [23, Introduction section] to have a brief overview on the possible reasons of nonuniqueness in inverse problems). In [24] and [25], the condition on the minimum number of independent data which ensures uniqueness of solution up to the cited trivial ambiguities is shown.

As concerns the choice of a procedure to search the solution, in the past, many methods have been introduced and a large part of them exploits the amplitude of Fourier transform of the unknown signal as data. The most famous of this class are the algorithms of Gerchberg and Saxton [26], Fienup [27], [28], and their variations [29], which are based on alternating projections. Despite their diffusion and their simplicity, these kinds of procedures have various drawbacks. The first one resides in *a priori* information about the unknown signal that are required by such algorithms but which may not be available. The second drawback can derive from the projections; in fact, if the projections are done onto non convex sets, these algorithms may not give a reasonable solution leaving open questions related to their convergence (except for the resampling version shown in [30]).

For all the previous reasons, it is worth investigating other approaches to tackle phase retrieval, and in this paper, we consider phase retrieval via lifting [2] and via quadratic inversion [3]. In particular, in Section II, we formalize the problem. In Sections III and IV, we illustrate phaselift and phase

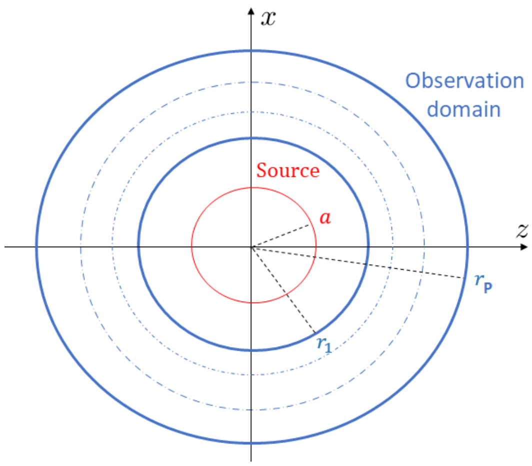

Fig. 1. Source domain and observation domain.

retrieval via quadratic inversion, respectively. In Section V, we provide numerical results for both methods. Finally, in Section VI, we make a comparison between the two approaches.

II. Statement of the Problem

In this paper, we consider the problem of determining the field radiated by a monochromatic electric current defined within a cylinder of radius a when M observations of square amplitude of such a field are collected over P circles external to the source. In particular, we refer to the 2-D and scalar geometry depicted in Fig. 1.

The electric source is assumed to be directed along the y-axis, which is also the axis of invariance of the configuration. The radii of each observation circle are denoted by $r_1, r_2, \ldots, r_P$, and on each circle, the square amplitude of the radiated field is sampled with a uniform angular step at M_0 points.

For the considered source, the radiated field E can be expressed as a truncated series of cylindric harmonics [31], therefore,

$$E(\rho, \varphi) \approx \sum_{n=-N_0}^{N_0} c_n H_n^2(\beta\rho) e^{jn\varphi} \tag{2}$$

where β is the free space wavenumber, $H_n^2(\cdot)$ is the nth-order Hankel function of second kind, and N_0 is the integer nearest to βa.

Hence, from the mathematical point of view, the problem of reconstructing the radiated field from the square amplitude observations of such a field consists in retrieving the unknown vector $\underline{x}$ from the set of phase-retrieval equations expressed by (1). Fixed $N = 2N_0 + 1$, in our case, it results that

1) $\underline{a}_m \in \mathbb{C}^N$ is the column vector which contains the sequence $\{(H_n^2(\beta\rho_m)e^{jn\varphi_m})^*\}_{n=-N_0}^{N_0}$, where $(\cdot)^*$ indicates the conjugate of $(\cdot)$;
2) $\underline{x} \in \mathcal{C}^N$ is the column vector which contains the unknown sequence $\{c_n\}_{n=-N_0}^{N_0}$; and
3) $b_m = |E(\rho_m, \varphi_m)|^2$ is the collected data in the mth point of sampling.

Because on each observation circle $M_0 = 4N_0 + 1$ square amplitude samples of radiated field are collected, it results that $\rho_m = r_p$ and $\varphi_m = [m - (p-1)M_0](2\pi/M_0)$ if $m \in [1 + \text{(p-1)}M_0,\ pM_0]$ with $p \in \{1, 2, \ldots, P\}$ indicating the considered circle. Let us point out that (2) can be used to span any 2-D scalar field; therefore, the mathematical model is the same even if we want to describe the field radiated by bidimensional sources closer to applications like the parabolic cylindrical reflector antenna. In order to recover $\underline{x}$ up to trivial ambiguities, we will illustrate and compare two different approaches to the phase retrieval problem:

1) *phaselift*;
2) *quadratic inversion*.

Although in this paper such methods are tested only with reference to the problem of recovering the field radiated by a 2-D scalar source, the applicability range of the two methods is very wide. The two methods, in fact, can be used every time that a basis of the finite-dimensional functional space of the radiated field is known. In [32]–[34], the basis that allows to span the field radiated by a strip current and that one of the field radiated by a source defined in a sphere (3-D geometry) are provided.

III. Phase Retrieval via PhaseLift

In this section, we describe a recent methodology for phase retrieval problem called *PhaseLift* which is based on a trace minimization problem for a matrix that is the solution of a linear system. This method was introduced in [35] and it was used for the first time in electromagnetic applications in [36] and [37]. At first, the PhaseLift paradigm uses the *lifting technique* to recast the phase-retrieval problem as a linear problem [2]. The lifting technique is based on the following equation:

$$\left|\underline{a}_m^H \underline{x}\right|^2 = Tr(\underline{\underline{A}}_m \underline{\underline{X}}) \quad \forall m \in \{1, \ldots, M\} \tag{3}$$

where $\underline{\underline{A}}_m = \underline{a}_m \underline{a}_m^H \in \mathcal{C}^{N\times N}$ and $\underline{\underline{X}} = \underline{x}\,\underline{x}^H \in \mathcal{C}^{N\times N}$. Equation (3) allows to lift up the unknown of phase retrieval problem in a space with a higher size in exchange for the linearity of the equations system to be solved; in fact, it permits to recast the problem of recovering the vector $\underline{x} \in \mathcal{C}^N$ from the quadratic constraints

$$\left|\underline{a}_m^H \underline{x}\right|^2 = b_m \quad \forall m \in \{1, \ldots, M\} \tag{4}$$

into the one of recovering the matrix $\underline{\underline{X}}$ from the set of linear equations

$$Tr(\underline{\underline{A}}_m \underline{\underline{X}}) = b_m \quad \forall m \in \{1, \ldots, M\}. \tag{5}$$

By introducing the linear operator

$$\mathcal{A}(\underline{\underline{X}}) = \{Tr(\underline{\underline{A}}_1 \underline{\underline{X}}), \ldots, Tr(\underline{\underline{A}}_M \underline{\underline{X}})\} \tag{6}$$

(which is also called *lifted operator*), the set of linear equations (5) can be expressed also in the following manner:

$$\mathcal{A}(\underline{\underline{X}}) = \underline{b} \tag{7}$$

where $\underline{b} = [b_1, b_2, \ldots, b_M]^T \in \mathcal{R}^M$ is the vector that contains the observed data. In order to estimate the solution $\underline{x}$ up to trivial ambiguities using only the lifting technique, the number of linearly independent equations must be equal to the number of unknowns and the coefficients matrix of linear system (7) must be well conditioned. However, because the phase retrieval problem after lifting could become highly undetermined [38], this approach is not always feasible. For this reason, Candes *et al.* [35] suggest adding some constraints to linear system (7). Such constraints involve the properties of unknown matrix $\underline{\underline{X}}$, and in fact, since the unknown matrix $\underline{\underline{X}}$ is an hermitian, positive semidefinite matrix with rank 1, the authors propose to tackle the following minimization:

$$min\ rank(\underline{\underline{X}})\quad s.t.\ \mathcal{A}(\underline{\underline{X}}) = \underline{b},\ \ \underline{\underline{X}} \succeq 0. \tag{8}$$

The previous problem is a nonconvex optimization that falls in the field of low rank matrix recovery, a class of optimization problems which has gained a lot of interest over the last few years [39]. The rank minimization is NP-hard but it can be relaxed into a convenient convex optimization called *PhaseLift* which consists in

$$min\ Tr(\underline{\underline{X}})\quad s.t.\ \mathcal{A}(\underline{\underline{X}}) = \underline{b},\ \ \underline{\underline{X}} \succeq 0. \tag{9}$$

In general, problems (8) and (9) do not have the same solutions, but when the linear operator $\mathcal{A}(\underline{\underline{X}})$ satisfies the restricted isometry property shown in [40], the two optimization problems are equivalent from the point of view of the solution. Such equivalence is based on the equality of the solution of l_0- and l_1-norm minimization, and in fact, the rank and the trace of a square matrix represent the l_0- and l_1-norms of the eigenvalues vector, respectively. In order to solve the problem (9), we must find the minimum of the functional

$$g(\underline{\underline{X}}) = \|\mathcal{A}(\underline{\underline{X}}) - \underline{b}\|_2^2 + \gamma\, Tr(\underline{\underline{X}})\quad s.t.\ \underline{\underline{X}} \succeq 0 \tag{10}$$

where $\|\cdot\|_2^2$ is the square of l_2-norm in data space ($\mathcal{R}^M$), and γ is a regularization parameter whose value depends on the noise level. The minimum of functional (10) can be searched by using a projected gradient method. By starting from an initial guess $\underline{\underline{X}}^{(0)}$, this iterative method defines

$$\underline{\underline{X}}^{(j+1)} = \mathcal{P}(\underline{\underline{X}}^{(j)} - t^{(j)}\nabla g|_{\underline{\underline{X}}^{(j)}}) \tag{11}$$

where ∇g is the gradient of the functional (10), $t^{(j)}$ is the stepsize of the minimization scheme, and $\mathcal{P}$ is an operator that dumps the negative eigenvalues realizing the projection in the space of positive semidefinite matrix.

The stepsize $t^{(j)}$ describes of how far the minimization scheme (starting from $\underline{\underline{X}}^{(j)}$) moves in the direction opposite to $\nabla g|_{\underline{\underline{X}}^{(j)}}$ which is also the direction of maximum descent. In order to increase the convergence speed, the stepsize is chosen according to an exact line search. The latter permits finding the optimal stepsize $t_{opt}^{(j)}$ which satisfies the condition

$$t_{opt}{}^{(j)} = \underset{t^{(j)}}{argmin}\ g(\underline{\underline{X}}^{(j)} - t^{(j)}\nabla g|_{\underline{\underline{X}}^{(j)}}). \tag{12}$$

The projector $\mathcal{P}$ is defined as

$$\mathcal{P}(\underline{\underline{X}}) = \sum_{n=1}^{N} max(\lambda_n, 0)\underline{u}_n\underline{u}_n^H \tag{13}$$

where $\sum_{n=1}^{N}\lambda_n\underline{u}_n\underline{u}_n^H$ is the eigenvalues decomposition of matrix $\underline{\underline{X}}$. In Appendix A, we illustrate how the minimization

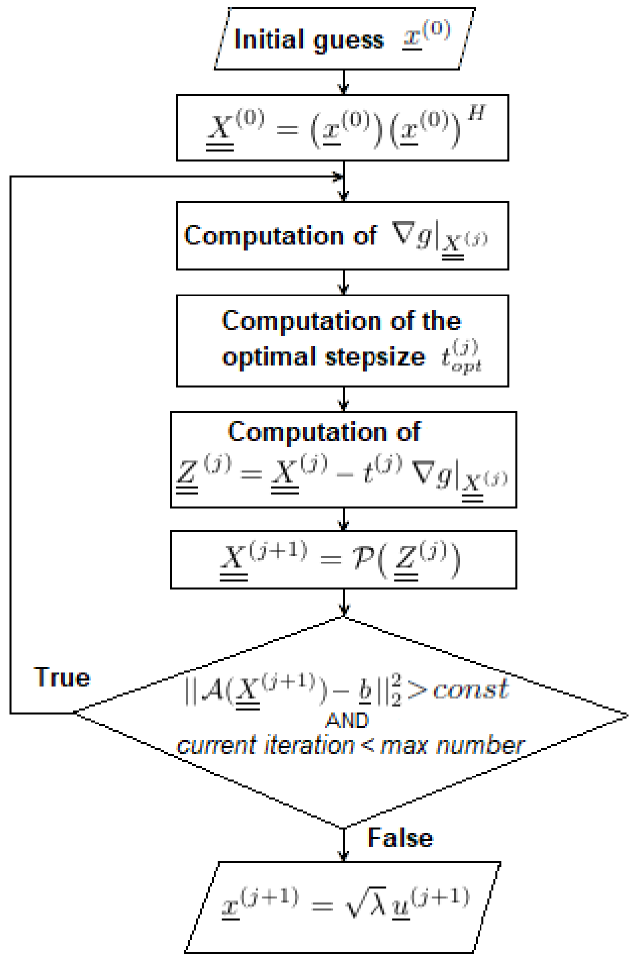

Fig. 2. Flowchart of the PhaseLift algorithm.

of functional (10), which in this section is described theoretically, can be implemented. Once the unknown matrix $\underline{\underline{X}}$ has been found, noting that $\underline{\underline{X}} = \underline{x}\ \underline{x}^H = \lambda\underline{u}\ \underline{u}^H$, the vector $\underline{x}$ can be reconstructed using the equation $\underline{x} = \sqrt{\lambda}\underline{u}$, where λ and $\underline{u}$ are, respectively, the only eigenvalue and the only eigenvector of $\underline{\underline{X}}$. In Fig. 2, the flowchart of the PhaseLift algorithm is shown.

IV. Phase Retrieval via Quadratic Inversion

The second method used in this paper to tackle the phase retrieval problem was introduced in [3] and recently reconsidered in [41] and [42]. This method is based on the inversion of the quadratic operator $\mathcal{B}(\underline{x}) = \{|\underline{a}_m^H\underline{x}|^2 : m = 1, 2, \ldots, M\}$ relating the unknown vector $\underline{x}$ to the vector of data $\underline{b}$. Such inversion is done by minimizing with respect to vector $\underline{x} \in \mathcal{C}^N$ the functional $\phi : \underline{x} \in \mathcal{C}^N \longrightarrow \mathcal{R}$ defined as follows:

$$\phi(\underline{x}) = \frac{1}{2M}\|\mathcal{B}(\underline{x}) - \underline{b}\|_2^2. \tag{14}$$

Hence, the generalized solution $\underline{x}_{sol}$ up to trivial ambiguities can be expressed as $\underline{x}_{sol} = \underset{\underline{x}}{argmin}\ \phi(\underline{x})$. By exploiting the

l_2-norm definition, the functional $\phi(\underline{x})$ becomes

$$\phi(\underline{x}) = \frac{1}{2M}\sum_{m=1}^{M}\left(\left|\underline{a}_m^H \underline{x}\right|^2 - b_m\right)^2. \tag{15}$$

The considered functional can be minimized using a gradient-like technique which, starting from an initial guess $\underline{x}_0$, estimates the solution recurring to the iterative equation

$$\underline{x}^{(j+1)} = \underline{x}^{(j)} - \alpha^{(j)}\hat{\nabla}\phi(\underline{x})|_{\underline{x}=\underline{x}^{(j)}} \tag{16}$$

where $\hat{\nabla}\phi$ is the pseudogradient of the functional and $\alpha^{(j)}$ is the stepsize of the algorithm.

The pseudogradient $\hat{\nabla}\phi$ has the following expression:

$$\hat{\nabla}\phi(\underline{x}) = \frac{1}{M}\sum_{m=1}^{M}\left(\left|\underline{a}_m^H \underline{x}\right|^2 - b_m\right)\left(\underline{a}_m \underline{a}_m^H\right)\underline{x}. \tag{17}$$

The stepsize is chosen performing an exact line search, and, therefore, its value is optimal. From the mathematical point of view, the optimal stepsize $\alpha_{opt}^{(j)}$ is such that

$$\alpha_{opt}^{(j)} = \underset{\alpha^{(j)}}{argmin}\ \phi(\underline{x}^{(j)} - \alpha^{(j)}\hat{\nabla}\phi|_{\underline{x}^{(j)}}). \tag{18}$$

In Appendix B, we provide some details about the definition of the pseudogradient $\hat{\nabla}\phi$, whereas in [3] and [43], the reader can find further details about the computation of the optimal stepsize $\alpha_{opt}^{(j)}$.

In Fig. 3, the flowchart of the quadratic inversion method is shown.

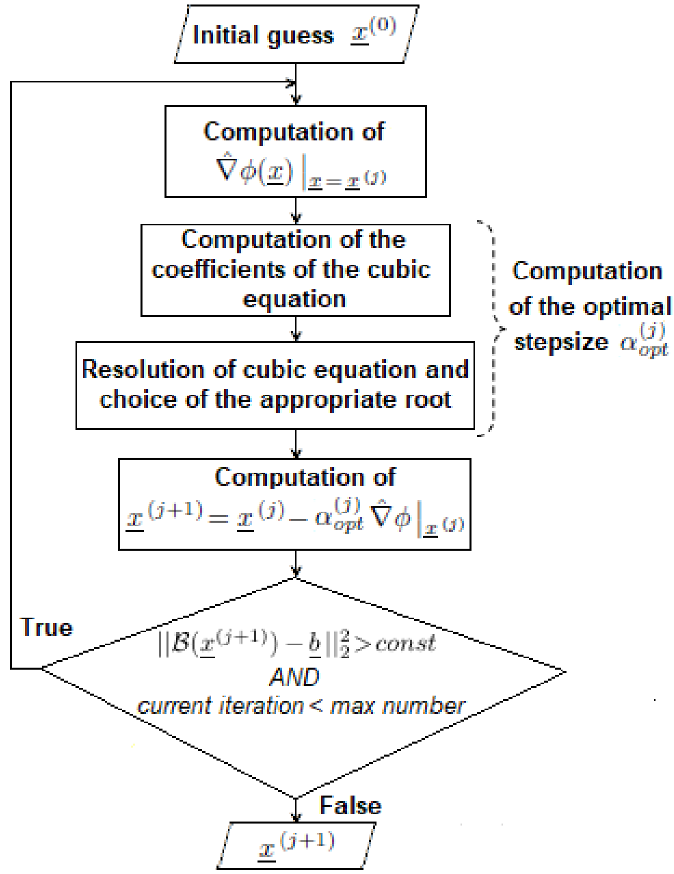

Fig. 3. Flowchart of the quadratic inversion method.

A. The Question of Local Minima

Since the functional $\phi(\underline{x})$ is quartic, the gradient descent scheme can trap in local minima which represent false solutions of the phase-retrieval problem. The presence of local minima is a big drawback, indeed, if the minimization scheme traps in a local minimum, the solution of the problem is not attainable. Moreover, the question is further complicated by the fact that iterative minimization methods (such as gradient descent) have only local validity and, therefore, they converge to the point of minimum nearest to initial guess $\underline{x}^{(0)}$.

In order to solve the question of local minima, many efforts have been done in [44]–[47]. In particular, Isernia *et al.* [44] provided the following sufficient condition which establishes the lack of a local minima along a considered direction. Let be $\underline{x}_{sol}$ the unknown solution of phase retrieval problem and $\Delta\underline{x} = \underline{x} - \underline{x}_{sol}$ a generic direction in unknown space. Departing from $\underline{x}_{sol}$ and moving along $\Delta\underline{x}$ direction, the values assumed by the functional ϕ are provided by the function

$$\phi(\lambda) = \phi(\underline{x}_{sol} + \lambda\Delta\underline{x}) = \frac{1}{2M}\lambda^2(a\lambda^2 + b\lambda + c) \tag{19}$$

where

1) $\lambda \in \mathcal{R}$ is a scalar which indicates the movement entity from the unknown solution $\underline{x}_{sol}$ along $\Delta\underline{x}$ direction;

2) a, b, and c are the scalars

$$a = \sum_{m=1}^{M}\left(\left|\underline{a}_m^H \Delta\underline{x}\right|^2\right)^2 \tag{20}$$

$$b = 4\sum_{m=1}^{M}\left|\underline{a}_m^H \Delta\underline{x}\right|^2 Re\left\{\left(\underline{a}_m^H \underline{x}_{sol}\right)^*\left(\underline{a}_m^H \Delta\underline{x}\right)\right\} \tag{21}$$

$$c = 4\sum_{m=1}^{M}\left(Re\left\{\left(\underline{a}_m^H \underline{x}_{sol}\right)^*\left(\underline{a}_m^H \Delta\underline{x}\right)\right\}\right)^2. \tag{22}$$

If $\lambda = 0$ is the only minimum point of $\phi(\lambda)$, then the functional $\phi(\underline{x})$ does not have local minima along the direction $\Delta\underline{x}$. Naturally, the previous condition is satisfied when $\phi'(\lambda) = 0$ only for $\lambda = 0$ and this occurs when the inequality

$$\frac{b^2}{ac} < \frac{32}{9} \tag{23}$$

is verified.

Observe that the constants a, b, and c are made up of M terms; in particular, the scalars a and c consist of positive terms only, whereas scalar b includes both positive and negative terms and, therefore, cancellation effects can arise in the computation of the scalar b.

At this point, let us analyze the dependence of the ratio (b^2/ac) from the number of independent data M_{ind} which can be defined as the number of "significant" singular values of

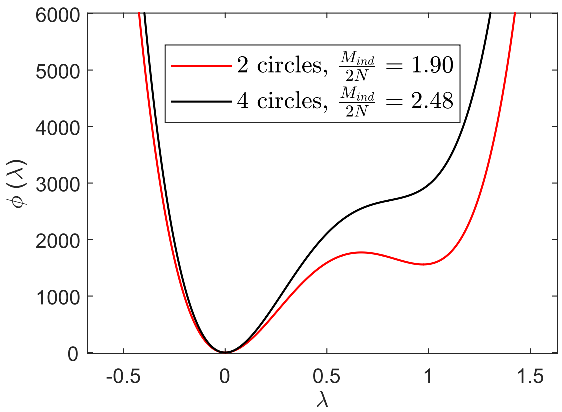

Fig. 4. Diagrams of the function $\phi(\lambda)$ along a specific direction $\Delta\underline{x}$ for two different values of independent data—unknowns' ratio. Diagrams refer to a source of radius $a = 1.9\lambda$ for two different observation domains. In the first case, the observation domain is an ensemble of two circles, whereas in the second case, it is an ensemble of four circles. On each circle are collected $4N_0 + 1 = 49$ measurements.

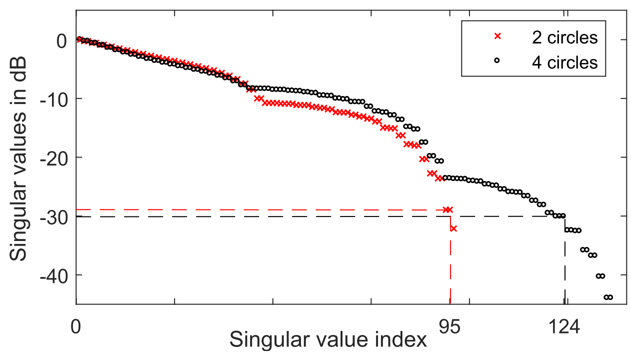

Fig. 5. Zoom-in view of singular values of the lifted operator for the evaluation of the number of independent data.

the lifted operator defined in (6). Having fixed the number of unknowns, if the number of independent data M_{ind} increases, then cancellation effects arise in the computation of b and consequently the ratio (b^2/ac) decreases. Therefore, for a sufficiently high value of the ratio

$$\frac{\textit{number of independent data}}{\textit{number of real unknowns}} = \frac{M_{ind}}{2N} \tag{24}$$

inequality (23) is satisfied for all the directions $\Delta\underline{x}$ that do not pass for the attraction region of the other global minima (due to ambiguity phase) and consequently the local minima of the functional $\phi(\underline{x})$ disappear [46]. From the topological point of view, the increase in independent data with respect to the number of real unknowns changes the structure of functional $\phi(\underline{x})$ making it gradually flatter. For the value of the ratio $(M_{ind}/2N)$ such that local minima disappear, phase retrieval via quadratic inversion becomes a globally convergent method.

Fig. 4 illustrates the function $\phi(\lambda)$ along a specific direction $\Delta\underline{x}$ for two different measurement setups or better for two different values of independent data—unknowns' ratio.

In order to allow an evaluation of the number of independent data for the example of Fig. 4, in Fig. 5 the significant singular values of lifted operator are shown.

TABLE I

Number of Observation Circles, Value of the Ratio $M_{ind}/2N$, and Value of the Ratio b^2/ac

Number of circles	$\frac{M_{ind}}{2N}$	$\frac{b^2}{ac}$
2	1.90	$3.8016 > 32/9$
4	2.48	$3.5120 < 32/9$

For the diagrams displayed in Fig. 4, Table I summarizes: the number of observation circles P, the value of ratio $(M_{ind}/2N)$, and the value of ratio (b^2/ac). As can be seen from Fig. 4, when measurements are collected only on two circles in addition to the absolute minimum, the function $\phi(\lambda)$ has also a relative minimum. Such a minimum disappears when measurements are collected on four circles because in such a case, the ratio $(M_{ind}/2N)$ is higher and the ratio (b^2/ac) satisfies the inequality (23).

V. Numerical Results

In order to show the performance of the two methods, the numerical results are provided. The accuracy of the numerical results will be quantified using the relative mean square error (rMSE) on reconstruction and on data. Because the solution of phase-retrieval problem can be recovered up to a global phase, in order to estimate the error on reconstruction it is necessary to normalize the unknown vector $\underline{x}$ and the reconstruction $\hat{\underline{x}}$ with respect to the phase of one of their elements. Hence, the rMSE on reconstruction in decibels has the following expression:

$$(rMSE_{reconstr})_{dB} = 10log_{10}\left(\frac{\|\hat{\underline{x}}_{norm} - \underline{x}_{norm}\|_2^2}{\|\underline{x}_{norm}\|_2^2}\right) \tag{25}$$

where $\underline{x}_{norm}$ and $\hat{\underline{x}}_{norm}$ are the normalized version of $\underline{x}$ and $\hat{\underline{x}}$, respectively. In this paper, the normalization of the vectors $\underline{x}$ and $\hat{\underline{x}}$ is done with respect to the phase of their first elements, consequently $\underline{x}_{norm} = (\underline{x}/e^{j\angle x_1})$ and $\hat{\underline{x}}_{norm} = (\hat{\underline{x}}/e^{j\angle \hat{x}_1})$. As concerns the rMSE on data in decibels, it is provided by

$$(rMSE_{data})_{dB} = 10log_{10}\left(\frac{\|\mathcal{B}(\hat{\underline{x}}) - \underline{b}\|_2^2}{\|\underline{b}\|_2^2}\right). \tag{26}$$

In test cases, the 2-D scalar current which is enclosed within a cylinder of radius $a = (N_0/\beta) = 1.9\lambda$ (where λ is the wavelength) is considered. The field radiated by such source is spanned by $N = 25$ Fourier–Bessel harmonics and the unknown coefficients of such harmonics are supposed to be given by the relation

$$c_n = 10e^{jn} \quad \forall n \in \{-12, -11, \ldots, 0, \ldots, 11, 12\}. \tag{27}$$

Both the approaches to the phase-retrieval problem will be tested in two different cases which differ in terms of the observation domain.

In the first case, the observation domain is an ensemble of two circles external to the source whose radii are, respectively, $\rho_1 = 3\lambda$ and $\rho_2 = 5\lambda$. On each circle, $M_0 = 4N_0 + 1 = 49$ observations with uniform angular step are collected; therefore, the total number of observations M is 98.

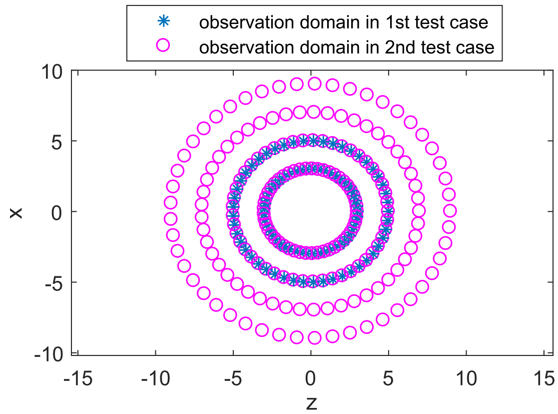

Fig. 6. Observation domain in both the test cases.

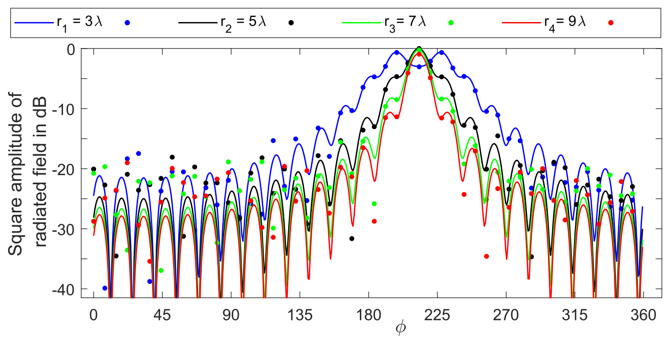

Fig. 7. Square amplitude of radiated field on observation circles and collected noisy data. Both the quantities are represented in decibels and normalized with respect to the maximum value.

In the second one, the observation domain is an ensemble of four circles whose radii are $\rho_1 = 3\lambda$, $\rho_2 = 5\lambda$, $\rho_3 = 7\lambda$, and $\rho_4 = 9\lambda$. The number of observations on each circle is unchanged with respect to the previous case; therefore, the total number M of observations is 196.

In Fig. 6, the observation domain of the first test case and that of the second test case are shown.

The data are corrupted by additive white Gaussian noise with a signal-to-noise ratio (SNR) equal to 30 dB. For both the approaches, the realization of noise is the same as in homologous simulation and the noise which corrupts data collected on first two circles of observations is the same in all the simulations.

In Fig. 7, the square amplitude of radiated field and collected data are depicted.

The initial guess $\underline{x}^{(0)} \in \mathcal{C}^{2N_0+1}$ is the same for all the simulations. It has been randomly chosen, in fact, both real and the imaginary parts of each component of $\underline{x}^{(0)}$ are realizations of uniform distributions supported on the set $[-20, 20]$.

The stop criteria is dictated by the noise level, and in fact, the iterative procedure is stopped as soon as the rMSE on data satisfies the inequality

$$(rMSE_{data})_{dB} \leq \left(\frac{\|\underline{n}\|_2^2}{\|\underline{b}\|_2^2}\right)_{dB} \tag{28}$$

where $\underline{n}$ is the noise which provides uncertainty on data and $\underline{b}$ is the vector of corrupted data.

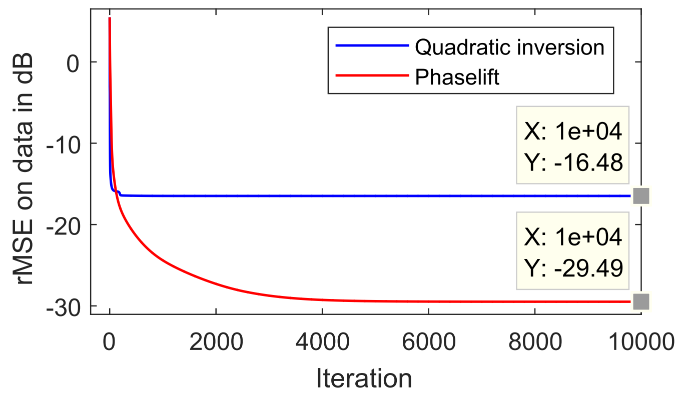

Fig. 8. Relative MSE on data in decibels with respect to the number of iterations when data are collected on two circles. Blue line: quadratic inversion. Red line: the PhaseLift paradigm.

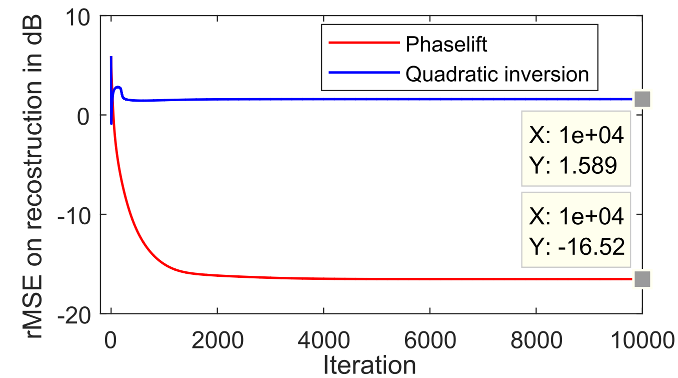

Fig. 9. Relative MSE on reconstruction in decibels with respect to the number of iterations when data are collected on two circles. Blue line: quadratic inversion. Red line: the PhaseLift paradigm.

In PhaseLift, the regularization parameter γ is chosen equal to 0.01. Such value has been obtained by using the criterion proposed in [49].

A. Simulations With Two Circles of Observation

In this section, the results of the simulations based on quadratic inversion and PhaseLift in the case of two circles of observations are provided.

In Fig. 8, the rMSE on data in decibels in terms of the number of iterations is sketched.

For both the approaches, the rMSE on data with respect to the number of iterations decreases and at the last iteration, it is equal to -16.48 dB for quadratic inversion and equal to -29.49 dB for PhaseLift. Nevertheless, because the limit value $(\|\underline{n}\|^2/\|\underline{b}\|^2)_{dB} = -31.02$ dB is not reached, the iterative procedure is stopped when the maximum number of iterations (fixed equal to 10^4) is attained. In Fig. 9, the rMSE on reconstruction provided by the two methods is depicted.

As it can be seen from the figure, the quadratic inversion does not reach the solution of the problem, and in fact, at the last iteration, the rMSE on reconstruction is equal to 1.59 dB. The PhaseLift paradigm, instead, provides a reconstruction of the solution with an rMSE equal to 16.52 dB.

In Fig. 10, the reconstruction provided by PhaseLift paradigm is compared with the ideal solution.

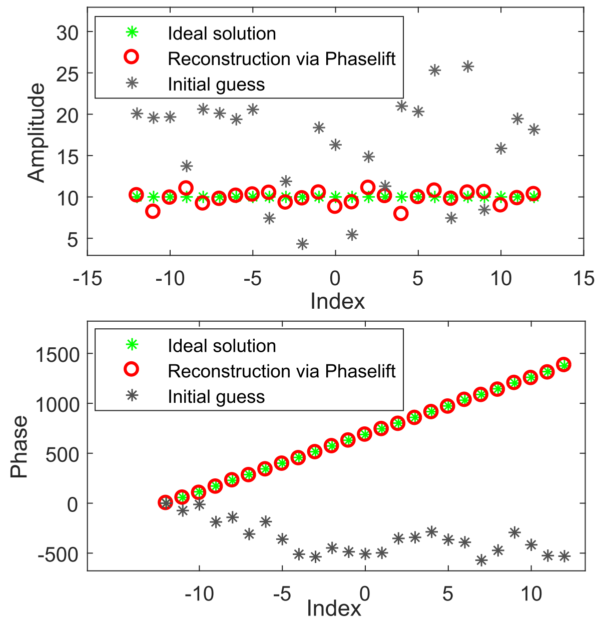

Fig. 10. Amplitude and phase diagrams of the ideal solution (in green), of the reconstruction via PhaseLift (in red), and of the initial guess (in grey).

TABLE II

ELABORATION TIME FOR A SINGLE ITERATION AND TOTAL TIME OF ELABORATION IN THE CASE OF TWO OBSERVATION CIRCLES

	Time for a single iteration	*Time for convergence*
Quadratic inversion	$5.30 \cdot 10^{-4}$ s	X
Phaselift	$3.50 \cdot 10^{-3}$ s	34.78 s

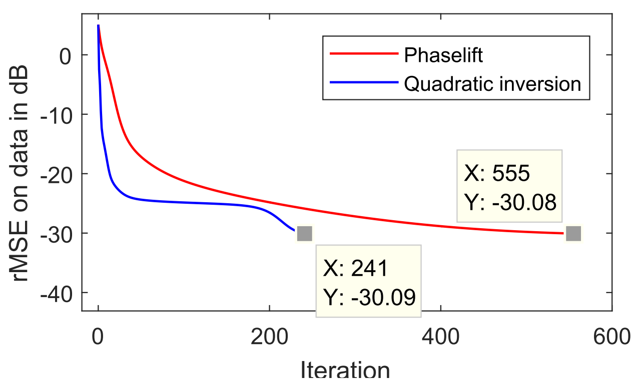

Fig. 11. Relative MSE on data with respect to the number of iterations when data are collected on four circles. Blue line: quadratic inversion. Red line: the PhaseLift paradigm.

As concerns the elaboration times, Table II shows the elaboration time of a single iteration and the total time of elaboration for both the approaches in the case of two observation circles. Simulations have been performed with the CPU AMD A12 9720P.

B. Simulations With Four Observation Circles

In this section, the results of the simulations based on quadratic inversion and PhaseLift in the case of four circles of observations are provided. In Fig. 11, the rMSE on data in decibels with respect to the number of iterations is sketched.

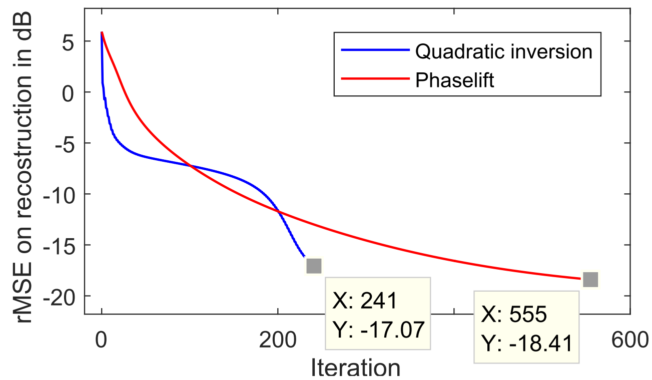

Fig. 12. Relative MSE on unknown with respect to the number of iterations when data are collected on four circles. Blue line: quadratic inversion. Red line: the PhaseLift paradigm.

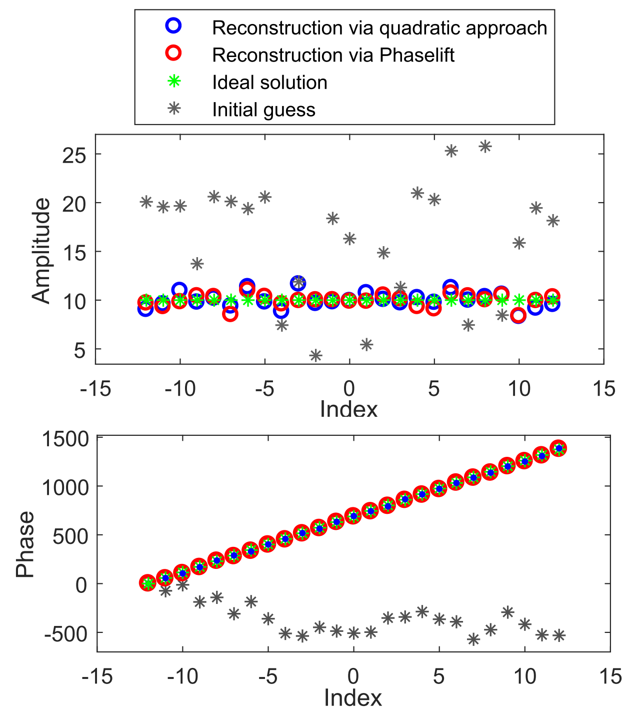

Fig. 13. Amplitude and phase diagrams of the ideal solution (in green), of the reconstruction via quadratic inversion (in blue), of the reconstruction via PhaseLift (in red), and of the initial guess (in grey).

In this case, both the approaches reach the limit value of rMSE on data which is equal to −30.08 dB, but in order to achieve this aim, the quadratic inversion requires 241 iterations, whereas PhaseLift requires 555 iterations. In Fig. 12, the rMSE on the reconstruction provided by the two methods is depicted.

As it can be seen from the previous figure, in this case, both approaches reach the solution of the problem, and in fact, quadratic inversion method estimates the solution with an rMSE equal to −17.07 dB, while PhaseLift estimates the solution with an rMSE equal to −18.41 dB.

In Fig. 13, the reconstructions provided by both approaches are compared with the ideal solution. Table III shows the computational time of a single iteration and the total elaboration time for both the approaches in the case of four observation circles.

TABLE III

ELABORATION TIME FOR A SINGLE ITERATION AND TOTAL TIME OF ELABORATION IN THE CASE OF FOUR OBSERVATION CIRCLES

	Time for one iteration	*Time for convergence*
Quadratic inversion	0.0013 s	0.319 s
Phaselift	0.0043 s	2.38 s

VI. Comparison of the Two Methods

On the basis of the numerical results of Section V, first we underline the role played by the ratio $(M_{ind}/2\ N)$ for both the approaches for phase retrieval and then we compare the two approaches. It is evident that passing from the measurement setup of Section V-A to the measurement setup of Section V-B, there is an increase in the ratio $(M_{ind}/2N)$ [38], [48]. As can be seen from the previous simulations, the increase in such ratio leads to benefits for both the approaches to phase retrieval, and in fact, for PhaseLift, the increase in the ratio $(M_{ind}/2N)$ entails a rise in the rate of convergence, while for quadratic inversion, the increase in such ratio makes the functional free of local minima and quasi-flat region in which the method can trap.

Before comparing the performances of both methods, it is useful to observe that in the quadratic inversion, the unknown is a vector of size N, while in the PhaseLift paradigm, the unknown is a matrix of size $N \times N$; for this reason, the memory requirements of the quadratic inversion are far lower than those necessary for the PhaseLift paradigm. Consequently, when the dimension of unknown vector $\underline{x}$ reaches the tens of thousand of elements, PhaseLift becomes computationally prohibitive and de facto impractical for actual desktop computers.

From the comparison of the two methods, it is clear that when the ratio $(M_{ind}/2N)$ satisfies the uniqueness condition but it is not sufficiently high to ensure the absence of local minima and quasi-flat regions in the functional (14), PhaseLift is preferable to the quadratic inversion method because the latter can trap. Differently, when the ratio $(M_{ind}/2N)$ is high enough to ensure the absence of traps in the functional (14), then the quadratic inversion method is more appealing for the recovering of the solution because its computational time is surely lower.

Summarizing, when the number of unknowns is of the order of tens of thousand, only the quadratic approach can recover the solution. Differently, when the number of unknowns is lower, the choice of the best method essentially depends on the number of independent data. If the number of independent data is sufficient to avoid the presence of local minima, then the quadratic inversion is more appealing than PhaseLift because its elaboration time is lower, and instead, if the number of data is not so high, then only PhaseLift allows to recover the solution.

Appendix A
Minimization Details of PhaseLift

As has been seen in Section III, the PhaseLift paradigm requires addressing the minimization of functional (10) with the further constraint that the unknown matrix $\underline{\underline{X}}$ is positive semidefinite. In order to achieve this task, it is possible to perform a constrained minimization of the functional

$$g(\underline{x}_L) = \|\underline{\underline{A}}_L \underline{x}_L - \underline{b}\|_2^2 + \gamma\, \underline{c}^T \underline{x}_L \tag{29}$$

where

1) $\underline{\underline{A}}_L \in \mathbb{C}^{M\times N^2}$ is the matrix whose mth row is built up by reshaping the rows of $\underline{\underline{A}}_m = \underline{a}_m \underline{a}_m^H\ \forall m \in \{1, 2, \ldots, M\}$ in a unique row; therefore, it can be partitioned as follows:

$$\underline{\underline{A}}_L = [\underline{\underline{A}}_{L1}, \underline{\underline{A}}_{L2}, \underline{\underline{A}}_{L3}, \cdots, \underline{\underline{A}}_{LN}] \tag{30}$$

with $\underline{\underline{A}}_{Ln} \in \mathbb{C}^{M\times N}\ \forall n \in \{1, 2, \ldots, N\}$;

2) $\underline{x}_L \in \mathbb{C}^{N^2}$ is the unknown vector and it is built up by reshaping the columns of matrix $\underline{\underline{X}}$ in a unique column vector so

$$\underline{x}_L = [X_{11}, X_{21}, \ldots, X_{N1}, X_{12}, X_{22}, \ldots, X_{N2}, \ldots, X_{1N}, X_{2N}, \ldots, X_{NN}]^T; \tag{31}$$

3) $\underline{c} \in \mathbb{R}^{N^2}$ is the vector which contains 1 where the vector $\underline{x}_L$ contains the elements of diagonal of matrix $\underline{\underline{X}}$ and 0 in the other positions.

The implementation of the PhaseLift paradigm based on the minimization of the functional (29) is not efficient because all the elements of the matrix $\underline{\underline{X}}$ are considered as unknowns. By exploiting the hermitian property of matrix $\underline{\underline{X}}$ $(X_{ji} = X_{ij}^*)$, it is possible to halve the number of real unknowns, in fact, only the elements X_{ij} such that $i = j, \ldots, N$ and $j = 1, \ldots, N$ can be considered as unknowns. Hence, in order to halve the number of unknowns, we propose to rewrite the product $\underline{\underline{A}}_L \underline{x}_L$ in such way

$$\underline{\underline{A}}_L \underline{x}_L = \underline{\underline{F}}\, \underline{x}_{T1} + \underline{\underline{G}}\, \underline{x}_{T2} + \underline{\underline{H}}\, \underline{x}_D \tag{32}$$

where

1) $\underline{x}_{T1}, \underline{x}_{T2} \in \mathbb{C}^{(N^2-N/2)}$, and $\underline{x}_D \in \mathbb{R}^N$ are the vectors made up of the elements X_{ij} located, respectively, in the lower triangle, in the upper triangle, and on the diagonal of matrix $\underline{\underline{X}}$, therefore,

$$\underline{x}_{T1} = [X_{21}, \ldots, X_{N1}, X_{32}, \ldots, X_{N2}, \ldots, X_{43}, \ldots, X_{N3}, \ldots, X_{NN-1}]^T \tag{33}$$

$$\underline{x}_{T2} = [X_{12}, \ldots, X_{1N}, X_{23}, \ldots, X_{2N}, \ldots, X_{34}, \ldots, X_{3N}, \ldots, X_{N-1N}]^T \tag{34}$$

$$\underline{x}_D = [X_{11}, X_{22}, X_{33}, \ldots, X_{NN}]^T; \tag{35}$$

2) $\underline{\underline{F}}, \underline{\underline{G}} \in \mathbb{C}^{M\times(N^2-N/2)}$ and $\underline{\underline{H}} \in \mathbb{R}^{M\times N}$ are so defined

$$\underline{\underline{F}} = [\underline{A}_{L1}(2), \ldots, \underline{A}_{L1}(N), \underline{A}_{L2}(3), \ldots, \underline{A}_{L2}(N), \underline{A}_{L3}(4), \ldots, \underline{A}_{L3}(N), \ldots, \underline{A}_{LN-1}(N)] \tag{36}$$

$$\underline{\underline{G}} = [\underline{A}_{L2}(1), \ldots, \underline{A}_{LN}(1), \underline{A}_{L3}(2), \ldots, \underline{A}_{LN}(2), \underline{A}_{L4}(3), \ldots, \underline{A}_{LN}(3), \ldots, \underline{A}_{LN}(N-1)] \tag{37}$$

$$\underline{\underline{H}} = [\underline{A}_{L1}(1), \underline{A}_{L2}(2), \ldots, \underline{A}_{LN}(N)] \tag{38}$$

with $\underline{A}_{Ln}(j)$ indicating the jth column of $\underline{\underline{A}}_{Ln}$.

As a consequence of the hermitian property of the matrices $\underline{\underline{A}}_k$ and $\underline{\underline{X}}$, it results that $\underline{\underline{G}} = \underline{\underline{F}}^*$ and $\underline{x}_{T2} = \underline{x}_{T1}^*$, therefore,

$$\underline{\underline{A}}_L \underline{x}_L = \underline{\underline{F}}\ \underline{x}_{T1} + \underline{\underline{F}}^* \underline{x}_{T1}^* + \underline{\underline{H}}\ \underline{x}_D. \tag{39}$$

Taking in account (39) and noting that $\|\underline{x}_D\|_1 = \underline{c}^T \underline{x}_L$, it is possible to rewrite the functional (29) as follows:

$$g(\underline{x}_{T1}, \underline{x}_D) = \left\|\underline{\underline{F}}\ \underline{x}_{T1} + \underline{\underline{F}}^* \underline{x}_{T1}^* + \underline{\underline{H}}\ \underline{x}_D - \underline{b}\right\|_2^2 + \gamma \|\underline{x}_D\|_1. \tag{40}$$

Denoting with $\underline{x}_{Tr} = Re\{\underline{x}_{T1}\}$ and $\underline{x}_{Ti} = Im\{\underline{x}_{T1}\}$, we have

$$\begin{aligned} g(\underline{x}_{Tr}, \underline{x}_{Ti}, \underline{x}_D) = \big\|&(\underline{\underline{F}} + \underline{\underline{F}}^*)\underline{x}_{Tr} + j(\underline{\underline{F}} - \underline{\underline{F}}^*)\underline{x}_{Ti} \\ &+ \underline{\underline{H}}\ \underline{x}_D - \underline{b}\big\|_2^2 + \gamma \|\underline{x}_D\|_1. \end{aligned} \tag{41}$$

Fixing $\underline{x}_{Lri} = [\underline{x}_{Tr}, \underline{x}_{Ti}, \underline{x}_D]^T$, $\underline{d} = [\underline{0}, \underline{0}, \underline{1}]^T$, and $\underline{\underline{A}}_{Lri} = [(\underline{\underline{F}} + \underline{\underline{F}}^*), j(\underline{\underline{F}} - \underline{\underline{F}}^*), \underline{\underline{H}}]$, the functional g can be rewritten in the following form:

$$g(\underline{x}_{Lri}) = \|\underline{\underline{A}}_{Lri} \underline{x}_{Lri} - \underline{b}\|^2 + \gamma\, \underline{d}^T \underline{x}_{Lri}. \tag{42}$$

Note that all the quantities that appear in $g(\underline{x}_{Lri})$ consist of real elements, and in fact, $\underline{\underline{A}}_{Lri} \in \mathbb{R}^{M \times N^2}$, $\underline{x}_{Lri} \in \mathbb{R}^{N^2}$, $\underline{b} \in \mathbb{R}^M$, and $\underline{d} \in \mathbb{R}^{N^2}$. With respect to the minimization of functional (29), the implementation of the PhaseLift paradigm based on the minimization of the functional (42) halves the number of unknowns and consequently, the elaboration time and the memory requirements decrease.

APPENDIX B
PSEUDOGRADIENT AND OPTIMAL STEPSIZE IN QUADRATIC INVERSION

In this appendix we define and compute the pseudogradient of the objective functional $\phi(\underline{x})$. Since the functional $\phi(\underline{x})$ is not holomorphic with respect to $\underline{x}$, in the minimization of the functional ϕ, we use the pseudogradient $\hat{\nabla}\phi$ [3]. The latter can be defined in the following manner:

$$\hat{\nabla}\phi = \left(\frac{\partial \phi}{\partial \underline{x}}\right)^* = \begin{bmatrix} \dfrac{\partial \phi}{\partial x_1} \\ \vdots \\ \dfrac{\partial \phi}{\partial x_N} \end{bmatrix}^* \tag{43}$$

where $\forall n \in \{1, \ldots, N\}$ $(\partial \phi / \partial x_n)$ are the Wirtinger partial derivatives, and therefore,

$$\frac{\partial \phi}{\partial x_n} = \frac{1}{2}\left(\frac{\partial \phi}{\partial Re\{x_n\}} - j\frac{\partial \phi}{\partial Im\{x_n\}}\right). \tag{44}$$

REFERENCES

[1] L. Taylor, "The phase retrieval problem," *IEEE Trans. Antennas Propag.*, vol. AP-29, no. 2, pp. 386–391, Mar. 1981.

[2] T. Isernia, G. Leone, and R. Pierri, "The phase retrieval by a reference source," in *Antennas Propag. Soc. Int. Symp. AP-S. Dig.*, Jun. 1989, pp. 61–64.

[3] T. Isernia, G. Leone, and R. Pierri, "New approach to antenna testing from near field phaseless data: The cylindrical scanning," *IEE Proc. H-Microw., Antennas Propag.*, vol. 139, no. 4, pp. 363–368, Aug. 1992.

[4] G. Hislop, L. Li, and A. Hellicar, "Phase retrieval for millimeter- and submillimeter–wave imaging," *IEEE Trans. Antennas Propag.*, vol. 57, no. 1, pp. 286–290, Jan. 2009.

[5] A. F. Morabito, R. Palmeri, V. A. Morabito, A. R. Laganà, and T. Isernia, "Single-surface phaseless characterization of antennas via hierarchically ordered optimizations," *IEEE Trans. Antennas Propag.*, vol. 67, no. 1, pp. 461–474, Jan. 2019.

[6] G. Hislop, G. C. James, and A. Hellicar, "Phase retrieval of scattered fields," *IEEE Trans. Antennas Propag.*, vol. 55, no. 8, pp. 2332–2341, Aug. 2007.

[7] G. Schnattinger, C. Lopez, E. Kılıç, and T. F. Eibert, "Fast near-field far-field transformation for phaseless and irregular antenna measurement data," *Adv. Radio Sci.*, vol. 12, pp. 171–177, Jan. 2014.

[8] A. Paulus, J. Knapp, and T. F. Eibert, "Phaseless near-field far-field transformation utilizing combinations of probe signals," *IEEE Trans. Antennas Propag.*, vol. 65, no. 10, pp. 5492–5502, Oct. 2017.

[9] T. Brown, C. Narendra, C. Niu, and P. Mojabi, "On the use of electromagnetic inversion for near-field antenna measurements: A review," in *Proc. IEEE Conf. Antenna Meas. Appl. (CAMA)*, Sep. 2018, pp. 1–4.

[10] J. F. Alvarez and O. Breinbjerg, "A computational and experimental investigation of $\lambda/2$ and $\lambda/4$ sampling step in phaseless planar near-field measurements at 60 GHz," in *Proc. 12th Eur. Conf. Antennas Propag.*, Apr. 2018, p. 5.

[11] A. Arboleya, J. Laviada, J. Ala-Laurinaho, Y. Álvarez, F. Las-Heras, and A. V. Räisänen, "Phaseless characterization of broadband antennas," *IEEE Trans. Antennas Propag.*, vol. 64, no. 2, pp. 484–495, Feb. 2016.

[12] S. F. Razavi and Y. Rahmat-Samii, "Phaseless measurements over non-rectangular planar near-field systems without probe corotation," *IEEE Trans. Antennas Propag.*, vol. 61, no. 1, pp. 143–152, Jan. 2013.

[13] J. Laviada, A. Arboleya-Arboleya, Y. Alvarez-Lopez, C. Garcia-Gonzalez, and F. Las-Heras, "Phaseless synthetic aperture radar with efficient sampling for broadband near-field imaging: Theory and validation," *IEEE Trans. Antennas Propag.*, vol. 63, no. 2, pp. 573–584, Feb. 2015.

[14] A. Walther, "The question of phase retrieval in optics," *Opt. Acta*, vol. 10, no. 1, pp. 41–49, Jan. 1963.

[15] X. Wang, W. Chen, and X. Chen, "Optical encryption and authentication based on phase retrieval and sparsity constraints," *IEEE Photon. J.*, vol. 7, no. 2, Apr. 2015, Art. no. 7800310.

[16] A. Descloux *et al.*, "Combined multi-plane phase retrieval and super-resolution optical fluctuation imaging for 4D cell microscopy," *Nature Photon.*, vol. 12, no. 3, pp. 165–172, Feb. 2018.

[17] R. P. Millane, "Phase retrieval in crystallography and optics," *J. Opt. Soc. Amer. A, Opt. Image Sci.*, vol. 7, no. 3, pp. 394–411, 1990.

[18] H. A. Hauptman, "The phase problem of X-ray crystallography," *Rep. Progr. Phys.*, vol. 54, no. 11, pp. 1427–1454, Nov. 1991.

[19] J. C. Dainty and J. R. Fienup, "Phase retrieval and image reconstruction for astronomy," in *Image Recovery*, H. Stark, Ed. New York, NY, USA: Academic, 1987, pp. 231–275.

[20] J. C. H. Spence, "Diffractive (Lensless) imaging," in *Sciences Microscopy*, P. W. Hawkes and J. C. H. Spence, Eds. New York, NY, USA: Springer, 2007.

[21] J. Qian, C. Yang, A. Schirotzek, F. Maia, and S. Marchesini, "Efficient algorithms for ptychographic phase retrieval," *Inverse Problems Appl., Contemp. Math*, vol. 615, pp. 261–280, May 2014.

[22] A. N. Tichonov and V. Y. Arsenine, *Solutions of Ill-Posed Problems*. New York, NY, USA: Wiley, 1977.

[23] A. Afsari, A. M. Abbosh, and Y. Rahmat-Samii, "A rapid medical microwave tomography based on partial differential equations," *IEEE Trans. Antennas Propag.*, vol. 66, no. 10, pp. 5521–5535, Oct. 2018.

[24] T. Isernia, G. Leone, and R. Pierri, "A quadratic inverse problem: The phase retrieval," in *Inverse Methods in Action*. Berlin, Germany: Springer, 1990, pp. 285–291.

[25] A. Conca, D. Edidin, M. Hering, and C. Vinzant, "An algebraic characterization of injectivity in phase retrieval," *Appl. Comput. Harmon. Anal.*, vol. 38, no. 2, pp. 346–356, 2015.

[26] R. W. Gerchberg, "A practical algorithm for the determination of phase from image and diffraction plane pictures," *Optik*, vol. 35, no. 2, pp. 237–246, 1972.

[27] J. R. Fienup, "Reconstruction of an object from the modulus of its Fourier transform," *Opt. Lett.*, vol. 3, no. 1, pp. 27–29, Jul. 1978.

[28] J. R. Fienup, "Phase retrieval algorithms: A comparison," *Appl. Opt.*, vol. 21, no. 15, pp. 2758–2768, 1982.

[29] M. Butola, R. Sunaina, and K. Khare, "Phase retrieval with complexity guidance," *J. Opt. Soc. Amer. A, Opt. Image Sci.*, vol. 36, no. 2, pp. 202–211, 2019.

[30] P. Netrapalli, P. Jain, and S. Sanghavi, "Phase retrieval using alternating minimization," *IEEE Trans. Signal Process.*, vol. 63, no. 18, pp. 4814–4826, Sep. 2015.

[31] G. Leone, M. A. Maisto, and R. Pierri, "Application of inverse source reconstruction to conformal antennas synthesis," *IEEE Trans. Antennas Propag.*, vol. 66, no. 3, pp. 1436–1445, Mar. 2018.

[32] M. A. Maisto, R. Solimene, and R. Pierri, "Resolution limits in inverse source problem for strip currents not in Fresnel zone," *J. Opt. Soc. Amer. A, Opt. Image Sci.*, vol. 36, no. 5, pp. 826–833, 2019.

[33] Z. Xie, Y.-H. Zhang, S.-Y. He, and G.-Q. Zhu, "A novel method for source reconstruction based on spherical wave expansion and NF-FF transformation using amplitude-only data," *IEEE Trans. Antennas Propag.*, vol. 67, no. 7, pp. 4756–4767, Jul. 2019.

[34] O. M. Bucci, G. D'Elia, R. Pierri, and G. Leone, "Far-field computation from amplitude near-field data on two surfaces: Cylindrical case," *IEE Proc. H-Microw., Antennas Propag.*, vol. 139, no. 2, p. 143, Apr. 1992.

[35] E. J. Candes, Y. C. Eldar, T. Strohmer, and V. Voroninski, "Phase retrieval via matrix completion," *SIAM Rev.*, vol. 57, no. 2, pp. 225–251, 2015.

[36] B. Fuchs and L. L. Coq, "Excitation retrieval of microwave linear arrays from phaseless far-field data," *IEEE Trans. Antennas Propag.*, vol. 63, no. 2, pp. 748–754, Feb. 2015.

[37] M. A. Maisto, R. Moretta, R. Solimene, and R. Pierri, "Phaseless arrays diagnostic by phaselift in near zone: Numerical experiments," in *Proc. PIERS*, Saint Petersburg, Russia, May 2017, pp. 1217–1221.

[38] M. A. Maisto, R. Moretta, R. Solimene, and R. Pierri, "On the number of independent equations in phase retrieval problem: Numerical results in circular case," in *Proc. PIERS*, Toyama, Japan, Aug. 2018, pp. 392–395.

[39] M. A. Davenport and J. Romberg, "An overview of low-rank matrix recovery from incomplete observations," *IEEE J. Sel. Topics Signal Process.*, vol. 10, no. 4, pp. 608–622, Jun. 2016.

[40] A. Chai, M. Moscoso, and G. Papanicolaou, "Array imaging using intensity-only measurements," *Inverse Problems*, vol. 27, no. 1, Dec. 2010, Art. no. 015005.

[41] E. J. Candès, X. Li, and M. Soltanolkotabi, "Phase retrieval via wirtinger flow: Theory and algorithms," *IEEE Trans. Inf. Theory*, vol. 61, no. 4, pp. 1985–2007, Apr. 2015.

[42] Z. Wei, W. Chen, C.-W. Qiu, and X. Chen, "Conjugate gradient method for phase retrieval based on the Wirtinger derivative," *J. Opt. Soc. Amer. A, Opt. Image Sci.*, vol. 34, no. 5, pp. 708–712, 2017.

[43] X. Jiang, S. Rajan, and X. Liu, "Wirtinger flow method with optimal stepsize for phase retrieval," *IEEE Signal Process. Lett.*, vol. 23, no. 11, pp. 1627–1631, Nov. 2016.

[44] T. Isernia, F. Soldovieri, G. Leone, and R. Pierri, "On the local minima in phase reconstruction algorithms," *Radio Sci.*, vol. 31, no. 6, pp. 1887–1899, 1996.

[45] T. Isernia, G. Leone, and R. Pierr, "Radiation pattern evaluation from near-field intensities on planes," *IEEE Trans. Antennas Propag.*, vol. 44, no. 5, pp. 701–710, May 1996.

[46] F. Soldovieri, A. Liseno, G. D'Elia, and R. Pierri, "Global convergence of phase retrieval by quadratic approach," *IEEE Trans. Antennas Propag.*, vol. 53, no. 10, pp. 3135–3141, Oct. 2005.

[47] J. Sun, Q. Qing, and J. Wright, "A geometric analysis of phase retrieval," in *Proc. Int. Symp. Inf. Theory*, Jul. 2016, pp. 2379–2383.

[48] R. Solimene, M. A. Maisto, G. Romeo, and R. Pierri, "On the singular spectrum of the radiation operator for multiple and extended observation domains," *Int. J. Antennas Propag.*, vol. 2013, Jun. 2013, Art. no. 585238. [Online]. Available: https://www.hindawi.com/journals/ijap/2013/585238/cta/

[49] A. Afsari, A. M. Abbosh, and Y. Rahmat-Samii, "Modified born iterative method in medical electromagnetic tomography using magnetic field fluctuation contrast source operator," *IEEE Trans. Microw. Theory Techn.*, vol. 67, no. 1, pp. 454–463, Jan. 2019.

Raffaele Moretta received the M.S. degree *(summa cum laude)* in electronic engineering from the University of Campania Luigi Vanvitelli, Aversa, Italy, in 2018, where he is currently pursuing the Ph.D. degree with the Electromagnetic Fields Group.

His current research interests include inverse problems in electromagnetics with particular attention to phase retrieval.

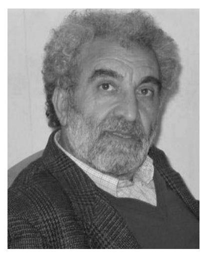

Rocco Pierri received the Laurea degree *(summa cum laude)* in electronic engineering from the University of Naples Federico II, Naples, Italy, in 1976.

He was with the University of Naples Federico II, Naples. He was a Visiting Scholar with the University of Illinois at Urbana–Champaign, Urbana, IL, USA; Harvard University, Cambridge, MA, USA; Northeastern University, Boston, MA, USA; Supelec, Paris, France; and the University of Leeds, Leeds, U.K. He also extensively lectured abroad in many universities and research centers. He is currently a Full Professor with the University of Campania Luigi Vanvitelli, Aversa, Italy. His current research interests include antennas, phase retrieval, near-field techniques, inverse electromagnetic scattering, subsurface sensing, electromagnetic diagnostics, microwave tomography, inverse source problems, and information content of radiated field.

Prof. Pierri was a recipient of the 1999 Honorable Mention for the H. A. Wheeler Applications Prize Paper Award of the IEEE Antennas and Propagation Society.